

# Search for $\gamma$ -rays following $\beta\beta$ decay of $^{100}\text{Mo}$ to excited states of $^{100}\text{Ru}$

NEMO Collaboration

D. Blum <sup>a</sup>, J. Busto <sup>a</sup>, J.E. Campagne <sup>a</sup>, D. Dassié <sup>b</sup>, F. Hubert <sup>b</sup>, Ph. Hubert <sup>b</sup>, M.C. Isaac <sup>b</sup>, C. Izac <sup>b</sup>, S. Jullian <sup>a</sup>, V.N. Kouts <sup>c</sup>, B.N. Kropivnyansky <sup>c</sup>, D. Lalanne <sup>a</sup>, T. Lamhamdi <sup>d</sup>, F. Laplanche <sup>a</sup>, F. Leccia <sup>b</sup>, I. Linck <sup>d</sup>, C. Longuemare <sup>c</sup>, P. Mennrath <sup>b</sup>, F. Natchez <sup>a</sup>, F. Scheibling <sup>d</sup>, G. Szklarz <sup>a</sup>, V.I. Tretyak <sup>c</sup> and Yu.G. Zdesenko <sup>c</sup>

<sup>a</sup> Laboratoire de l'Accélérateur Linéaire, IN2P3-CNRS et Université de Paris-Sud, F-91405 Orsay Cedex, France

<sup>b</sup> Centre d'Etudes Nucléaires, IN2P3-CNRS et Université de Bordeaux, F-33175 Gradignan Cedex, France

<sup>c</sup> Institute of Nuclear Research of the Ukrainian Academy of Sciences, SU-252 028 Kiev, USSR

<sup>d</sup> Centre de Recherches Nucléaires, IN2P3-CNRS et Université Louis Pasteur, F-67037 Strasbourg Cedex, France

<sup>e</sup> Laboratoire de Physique Corpusculaire, IN2P3-CNRS et Université de Caen, F-14032 Cean Cedex, France

Received 28 October 1991

An experiment looking for  $\beta\beta$  decay of  $^{100}\text{Mo}$  to excited states of  $^{100}\text{Ru}$  has been performed in the Fréjus Underground Laboratory. The used set-up included a high purity Ge detector and 1 kg of 99.5% enriched  $^{100}\text{Mo}$ . Half-life limits in the range  $10^{21}$  yr have been obtained.

## 1. Introduction

$0\nu\beta\beta$  decay experiments are nowadays well considered as a test of the standard electroweak model since an observation of this process would imply non-zero mass Majorana neutrinos, and possibly the existence of right-handed currents. For recent reviews see refs. [1–5]. However, the interpretation of any experimental result has to go through the complex problem of evaluating the nuclear matrix elements. In that way, experimental studies of  $2\nu\beta\beta$  decays are useful in order to check the different theoretical calculations.

Recently, new experimental results for the  $0^+ \rightarrow 0^+$   $2\nu\beta\beta$  decays have been published for  $^{82}\text{Se}$  [6],  $^{76}\text{Ge}$  [7], and  $^{100}\text{Mo}$  [8–10]. Among them the  $^{100}\text{Mo}$  has the shortest experimental half-life, around  $10^{19}$  yr. The decay scheme of  $^{100}\text{Mo}$  to the first levels of  $^{100}\text{Ru}$  is shown in fig. 1. Assuming about the same nuclear matrix elements for the  $0^+ \rightarrow 0_1^+$  and the  $0^+ \rightarrow 0^+$  decays and taking into account the phase space factors, we can expect a half-life of around  $10^{21}$  yr for the former transition. Such a half-life is accessible to  $\gamma$ -ray

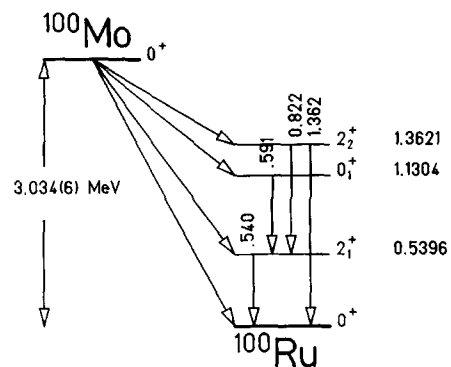


Fig. 1. Nuclear scheme for the  $\beta\beta$  decay in  $^{100}\text{Mo}$ . Energies are given in MeV. The  $Q_{\beta\beta}$  value of  $3.034 \pm 0.006$  MeV is taken from ref. [11].

spectroscopy when combining an ultra-low background Ge detector with a large amount of enriched  $^{100}\text{Mo}$ . So  $^{100}\text{Mo}$  is a good candidate for a search of  $2\nu\beta\beta$  decay to the  $0_1^+$  state. On the contrary, for the  $2\nu\beta\beta$  decay to the  $2^+$  excited states, the theoretical

estimations lead to longer half-lives by several orders of magnitudes [1,12,13].

This paper reports on a search for  $\gamma$ -rays following the  $\beta\beta$  decay of  $^{100}\text{Mo}$  to the excited states of  $^{100}\text{Ru}$ . The measurement has been carried out in the Fréjus Underground Laboratory with  $\approx 1$  kg sample of  $^{100}\text{Mo}$  enriched to 99.5%. Previous results for the  $\beta\beta$  decay of  $^{100}\text{Mo}$  to the excited states of  $^{100}\text{Ru}$  have already been published by Barabash et al. [14] and an improved experiment is now taking data [15].

## 2. Experimental set-up

The Ge spectrometer consists of a  $100\text{ cm}^3$  "p" type HPGe crystal [16]. A special effort was done to carefully select all detector components as well as shielding materials for their low level of intrinsic radioactivity. An extensive program was carried out for several months. The cryostat, endcaps of the crystal and different mechanical parts holding the assembly, were made of very pure Al-Si (4%) alloy with less than 0.3 ppt ( $10^{-12}$  g/g) of U and Th isotopes. No  $\gamma$ -activity from the Ra, Th and Tl isotopes of the natural chains was detectable in this alloy at the sensitivity level of 0.1 dpm/kg (decay per minute and per kilogram). Moreover, no  $\gamma$ -activities were found for the most common radioisotopes, namely  $^{137}\text{Cs}$  ( $<0.1$  dpm/kg),  $^{60}\text{Co}$  ( $<0.1$  dpm/kg) and  $^{40}\text{K}$  ( $<2.0$  dpm/kg).

The cryostat has a J-type geometry, and the pre-amplifier is set outside the shielding. The first stage of the preamplifier, made with selected J-FET and resistor and a homemade capacitor, is set inside the cryostat, 10 cm away from the Ge crystal. This has the advantage of keeping on the good energy resolution of standard Ge detectors. The passive shielding consists of 18 cm of OFHC copper inside 15 cm of ordinary lead.

Special care is taken to avoid a possible contamination by radon: no free space is left between the detector and the shielding, and a closed plastic sheet surrounds the lead shielding. In addition, in the Fréjus Underground Laboratory, a strong air ventilation keeps a constant low Rn activity of  $50\text{ Bq/m}^3$ .

Within these experimental conditions, the background counting rate is 10 counts/h for energies  $\geq 30$  keV. The main background components come from

$^{214}\text{Bi}$ ,  $^{214}\text{Pb}$ ,  $^{40}\text{K}$  and man-made or cosmogenic radioactivity,  $^{137}\text{Cs}$  and  $^{60}\text{Co}$ . Around 2 MeV the background level is 1.2 counts/keV kg yr.

The electronics consist of a currently available spectroscopic amplifier and a 8192 channel ADC. The energy calibration, adjusted with standard sources to 0.42 keV/channel, covers the energy range from 30 keV up to 3.5 MeV. The instantaneous energy resolution (FWHM) of the detector is 1.8 keV on the 1332 keV line of  $^{60}\text{Co}$ . Since the experiment was running for a long time, the stability of the electronic chain was checked periodically. For that purpose, we use the presence of  $^{40}\text{K}$  and  $^{137}\text{Cs}$  impurities in the  $^{100}\text{Mo}$  sample to get a self-calibration of the spectrum. The final energy resolution over 3 months of running time is 1.40 keV on the 661 keV line of  $^{137}\text{Cs}$  and 1.95 keV on the 1461 keV line of  $^{40}\text{K}$ . This stability of the electronics is mainly a consequence of the constant temperature ( $\approx 23^\circ\text{C}$ ) and the low hygrometric degree ( $\approx 50\%$ ) in the underground laboratory.

The  $\beta\beta$  source consists of a 994 g sample of metallic Mo powder enriched to 99.5% in  $^{100}\text{Mo}$ . A special container made of delrin was shaped in order to optimize the detector efficiency (Marinelli geometry) and to avoid any free space between the detector and the copper part of the shielding.

The efficiency of the detector has been calculated in the experimental conditions using different Monte Carlo codes. Taking into account the apparent density  $\rho = 1.0\text{ g/cm}^3$  of the powder, the efficiencies at the relevant energies of 540 keV, 591 keV, 822 keV, and 1362 keV are respectively 1.2%, 1.1%, 0.9%, and 0.6%. Errors on these values are  $\approx 10\%$ , and reflect the uncertainties in the geometrical characteristics of the Ge crystal and sample.

## 3. Analysis and results

The raw  $\gamma$ -ray spectrum recorded in 2298 h of running time with the  $^{100}\text{Mo}$  sample is shown in the upper part of figs. 2 and 3. During the data taking the integrated total number of counts, mainly given by the  $\gamma$  decay of the long-life impurities of the  $^{100}\text{Mo}$  sample, follow a linear behaviour as a function of time (as shown in fig. 4). Any deviation from this linear behaviour could have revealed spurious events due

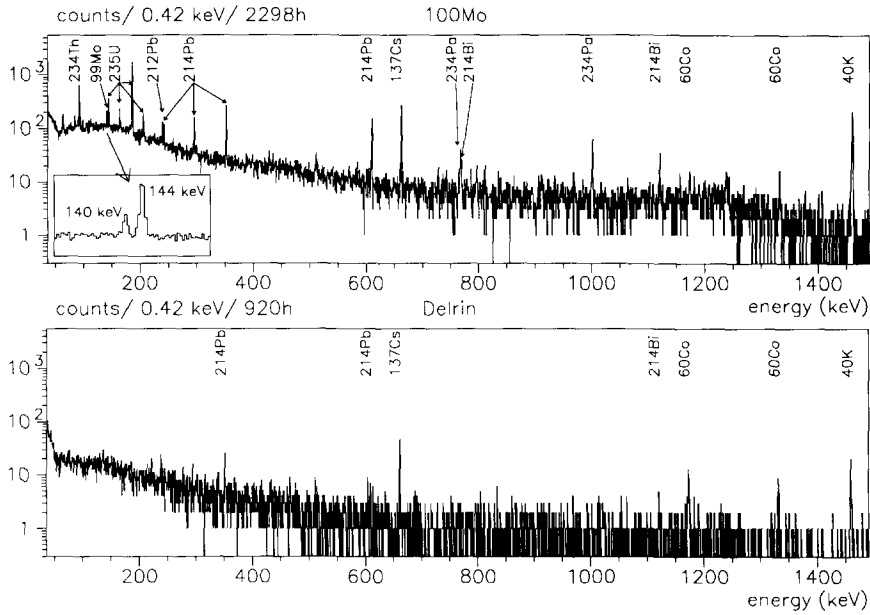


Fig. 2. Upper part: Low energy part of the  $\gamma$ -ray spectrum recorded in 2298 h in presence of the  $^{100}\text{Mo}$  sample. The insert shows the doublet at 140 keV ( $^{99}\text{Mo}$ ) and 144 keV ( $^{235}\text{U}$ ). Lower part: Low energy part of the  $\gamma$ -ray spectrum recorded in 920 h in presence of the plain delrin sample (cf. text).

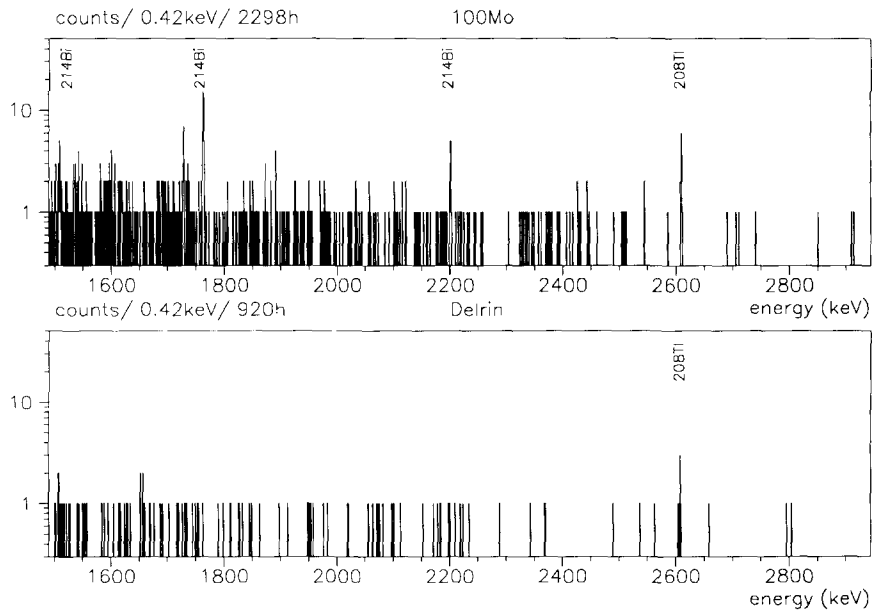


Fig. 3. The same as fig. 2 but for the high energy part of the spectra.

also found a weak activity of  $^{96}\text{Nb}$  ( $T_{1/2}=23$  h). The other activities, namely  $^{54}\text{Mn}$  (0.4 counts/d),  $^{58}\text{Co}$  (0.7 counts/d) and  $^{60}\text{Co}$  (0.8 counts/d), present in the spectrum come from the copper part of the shielding.

All the  $\gamma$ -ray lines observed in the final spectrum of figs. 2 and 3 are easily identified, showing some contaminations of the enriched  $^{100}\text{Mo}$  sample. Calculation of the different activities can be carried out if the actual background of the spectrometer is known. Notice that the true background is not easy to obtain since (i) any free space between the detector and the shielding will induce radon contamination, (ii) any material in this free space will add its own radioactivity, (iii) any material with a density and an atomic number different from those of the Mo sample will change the absorption of  $\gamma$ 's emitted from the shielding. As a compromise we chose to record a  $\gamma$ -ray spectrum with a 2.5 kg delrin sample similar in shape and volume to the Mo sample. The corresponding energy spectrum recorded in 920 h is shown in the lower part of figs. 2 and 3. The difficulty of having a good estimation of the background is illustrated by the spectrum, since we observed a slight contamination in  $^{134}\text{Cs}$  (0.012 dpm/kg),  $^{137}\text{Cs}$  (0.06 dpm/kg) and  $^{60}\text{Co}$  (0.04 dpm/kg) in the delrin sample.

Table 1 shows the contaminants together with the energy and area of their most intense  $\gamma$ -rays, measured in both Mo and delrin samples. The last column of table 1 gives the deduced activity in the Mo sample. Note the breaking of the secular equilibrium both in the  $^{238}\text{U}$  and  $^{235}\text{U}$  chains; in the  $^{235}\text{U}$  case the daughter isotope  $^{231}\text{Pa}$  has not even been observed.

The  $\gamma$ -ray spectra restricted to the energy ranges corresponding to the decay of the first excited states of  $^{100}\text{Ru}$ , respectively the  $2_1^+ \rightarrow 0^+$ ,  $0_1^+ \rightarrow 2_1^+$ ,  $2_2^+ \rightarrow 2_1^+$  and  $2_2^+ \rightarrow 0^+$  transitions (see fig. 1) are given in fig. 5. In these energy regions there are no visible peaks at the expected energy values. Upper limits on the peak areas have been extracted using the procedure of Helene [17,18]. Results are given in table 2, together with the half-life limits calculated using the following expression:

$$T_{1/2} \geq \log 2 \epsilon N_0 t r_\gamma / S,$$

where  $\epsilon$  is the detection efficiency of the  $\gamma$ -ray,  $N_0$  the number of  $^{100}\text{Mo}$  nuclei in the sample,  $t$  the running time (2298 h),  $r_\gamma$  the  $\gamma$  branching ratio and  $S$  the up-

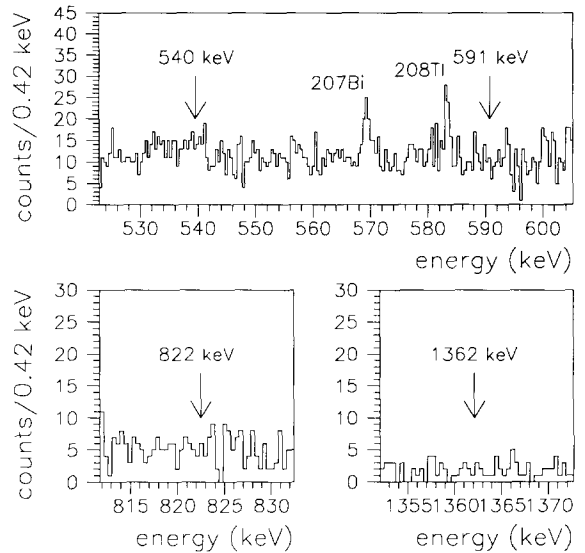


Fig. 5. Partial  $\gamma$ -ray spectra in the energy ranges corresponding to the decay of the first excited states of  $^{100}\text{Ru}$ . The arrows indicate the expected positions of the 540, 591, 822 and 1362 keV  $\gamma$ -ray lines which corresponds respectively to the  $2_1^+ \rightarrow 0^+$ ,  $0_1^+ \rightarrow 2_1^+$ ,  $2_2^+ \rightarrow 2_1^+$  and  $2_2^+ \rightarrow 0^+$  transitions in  $^{100}\text{Ru}$ .

per limit on the peak area. For comparison, the last results obtained by Barabash et al. [15] at 68% CL, are also given.

As already noted in the introduction, the  $0^+ \rightarrow 2_{1,2}^+$   $2\nu\beta\beta$  expected rates are lower by several orders of magnitude than the  $0^+ \rightarrow 0_1^+$   $2\nu\beta\beta$  transition rate. Therefore within the assumption that the two former transition rates are negligible, the two  $\gamma$ -ray transitions  $0_1^+ \rightarrow 2_1^+$  and  $2_1^+ \rightarrow 0^+$  deexciting the  $0_1^+$  state in  $^{100}\text{Ru}$  have been analysed simultaneously. Two different ways have been used, first summing the two corresponding energy bins around 540 and 591 keV and second multiplying the two individual probability density functions [17]. These two analyses lead to similar results, i.e., a  $0^+ \rightarrow 0_1^+$   $2\nu\beta\beta$  decay half-life limit  $T_{1/2} \geq 1.2 \times 10^{21}$  yr (90% CL), larger than the value given in table 2.

The present experimental sensitivity is close to the reasonable expectations for  $T_{1/2}^{2\nu\beta\beta}(0^+ \rightarrow 0_1^+)$ . But since only a lower limit has been obtained, it is worthwhile looking for further improvements in the sensitivity. One possibility is to increase the efficiency through the use of a larger volume Ge detector. This has the other advantage of decreasing the continuous back-

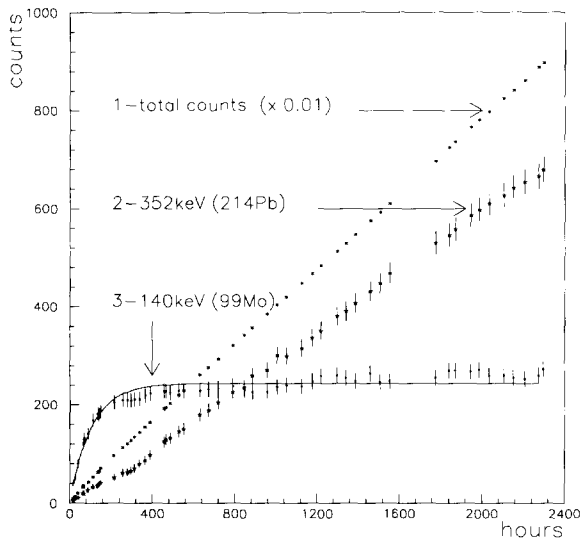


Fig. 4. Integrated number of counts as a function of time.

for example to parasitic electronic pulses or to microphonic pulses. In the same way the counting rates of all observed lines were continuously monitored. For example the 352 keV line of the  $^{214}\text{Pb}$  radioisotope can be populated either from the long-life  $^{226}\text{Ra}$  ( $T_{1/2} = 1600$  yr) impurity in the different materials, or from the short-life  $^{222}\text{Rn}$  ( $T_{1/2} = 3.8$  d) in the air. Therefore, the observed behaviour (fig. 4) of its  $\gamma$ -decay intensity tells us that no  $^{222}\text{Rn}$  pollution is visible in our experimental set-up. Finally, fig. 4 shows also the time evolution of the 140 keV peak intensity from the  $^{99}\text{Mo}$  cosmogenic isotope. A fit of the integrated number of counts leads to a half-life of  $T_{1/2} = 62 \pm 4$  h, in agreement with the known value of  $T_{1/2} = 66$  h. This radioisotope was activated by the cosmic rays through the  $^{100}\text{Mo}(n, 2n)$  and  $(p, d)$  reactions, before the sample was brought into the underground laboratory. Using the same procedure we

Table 1

Activity measurements of the  $^{100}\text{Mo}$  sample for the three natural chains and for the most common radioisotopes. Limits on the area are given at 68% CL. The last column gives the activity in disintegration per minute per kilogram (dpm/kg) for the  $^{100}\text{Mo}$  sample taking into account the background obtained from the delrin measurement. Numbers in parenthesis give the uncertainties on the last digit(s).

	Isotope	$\gamma$ line (keV)	Peak area (counts)		Activity $^{100}\text{Mo}$ (dpm/kg)
			$^{100}\text{Mo}$ 2298 h	delrin 920 h	
$^{232}\text{Th}$ family	$^{228}\text{Ac}$	969	26	<3	0.14(4)
	$^{212}\text{Pb}$	239	244	41	0.12(3)
	$^{208}\text{Tl}^a$	583	41	<3	0.03(1)
		2614	23	8	<0.03
$^{238}\text{U}$ family	$^{234}\text{Th}$	93	1600	<10	26(10)
	$^{234}\text{Pa}^m$	1001	255	<3	37(10)
	$^{214}\text{Pb}$	242	185	10	0.71(13)
		295	379	34	0.59(10)
		352	682	58	0.64(10)
	$^{214}\text{Bi}$	609	549	32	0.68(10)
		1120	98	10	0.51(13)
1764		90	<3	0.80(16)	
$^{235}\text{U}$ family	$^{235}\text{U}$	144	752	<10	2.3(3)
		163	359	<10	2.2(3)
		186	4276	<10	2.3(3)
		205	337	<10	2.0(3)
	$^{40}\text{K}$	1461	1058	81	11(2)
	$^{60}\text{Co}^b$	1173	76	64	<0.02
		1332	67	57	<0.02
	$^{137}\text{Cs}^b$	661	1006	179	0.46(8)
	$^{207}\text{Bi}$	569	46	<3	0.03(1)
		1063	22	<3	0.03(1)

<sup>a)</sup> Note that the branching ratio  $^{212}\text{Pb} \rightarrow ^{208}\text{Tl}$  is only 36.2%.

<sup>b)</sup> For these isotopes corrections have been made taking into account the delrin contamination.

Table 2

Limits on the half-lives of  $^{100}\text{Mo}$  for the  $2\nu\beta\beta$  transitions to the excited states of  $^{100}\text{Ru}$ . Within the assumption that the  $0^+ \rightarrow 2^+_{1,2}$   $2\nu\beta\beta$  decays are negligible, a simultaneous analysis of the two  $\gamma$ -ray transitions  $0^+ \rightarrow 2^+_{1,2}$  and  $2^+_{1,2} \rightarrow 0^+$  deexciting the  $0^+_{1,2}$  state in  $^{100}\text{Ru}$  (590.8 and 539.6 keV respectively) leads to a  $0^+ \rightarrow 0^+_{1,2}$   $2\nu\beta\beta$  decay half-life limit  $T_{1/2} \geq 1.2 \times 10^{21}$  yr (90% CL).

$\beta\beta$ transition	$E_\gamma$ (keV)	Upper limit of peak area (counts)		Half-life limit ( $\times 10^{21}$ yr)		
		90% CL	68% CL	present work		ref. [15] 68% CL
				90% CL	68% CL	
$0^+ \rightarrow 2^+_{1,2}$	539.6	$\leq 25$	$\leq 18$	$\geq 0.5$	$\geq 0.7$	$\geq 0.8$
$0^+ \rightarrow 0^+_{1,2}$	590.8	$\leq 13$	$\leq 8$	$\geq 0.9$	$\geq 1.5$	$\geq 0.5$
$0^+ \rightarrow 2^+_{1,2}$	822.5	$\leq 9$	$\leq 5$	$\geq 0.6$	$\geq 1.0$	
$0^+ \rightarrow 2^+_{1,2}$	1362.1	$\leq 8$	$\leq 5$	$\geq 0.4$	$\geq 0.6$	$\geq 0.4$

ground by increasing the peak/Compton ratio. A second possibility is to decrease the continuous background around 591 keV. This becomes more evident if we note that the average background at 591 keV in the present experiment is around 200 counts/keV kg yr, while the background of our Ge detector with the delrin sample at this energy is 6 times less. As shown in fig. 2, it is clear that the main component of this background comes from the Compton spectrum induced by the rather strong  $^{40}\text{K}$  contaminant of the  $^{100}\text{Mo}$  sample. Taking away this  $^{40}\text{K}$  pollution using some chemical process would lower the background significantly. Finally, there exist still possibilities to increase the amount of the  $^{100}\text{Mo}$  sample and the running time. All together a sensitivity of  $10^{22}$  yr or higher could be obtained.

### Acknowledgement

The authors would like to thank the Fréjus Underground Laboratory staff for their technical assistance when running the experiment. Special thanks go to O. Helene for discussions of the data analysis.

### References

- [1] T. Tomoda, Rep. Prog. Phys. 54 (1991) 53.
- [2] K. Muto and H.V. Klapdor, in: Neutrinos, ed. H.V. Klapdor (Springer, Berlin, 1988) pp. 183–237.
- [3] F.T. Avignone III and R.L. Brodzinsky, Prog. Part. Nucl. Phys. 21 (1988) 99.
- [4] M.K. Moe, Nucl. Phys. B (Proc. Suppl.) 19 (1991) 158.
- [5] A.S. Barabash, in: Proc. Intern. Symp. on Weak and electromagnetic interactions in nuclei (WEIN 89) (Montreal, 1989) ed. P. Depommier (Editions Frontières, Gif-sur-Yvette, France).
- [6] S.R. Elliott, A.A. Hahn and M.K. Moe, Phys. Rev. Lett. 59 (1987) 2020.
- [7] F.T. Avignone III et al., Phys. Lett. B 256 (1991) 559.
- [8] S.R. Elliott et al., 14th European Conf. on Nuclear physics: Rare nuclear decays and fundamental processes (Bratislava, Czechoslovakia, October 1990).
- [9] H. Ejiri et al., Phys. Lett. B 258 (1991) 17.
- [10] A.A. Klimenko et al., Proc. 1st Intern. Workshop on Theoretical and phenomenological aspects on underground physics (TAUP '89) (University of l'Aquila and Gran Sasso Laboratory, Italy, September 1989).
- [11] A.H. Wapstra and G. Audi, Nucl. Phys. A 432 (1985) 55.
- [12] W.C. Haxton and G.J. Stephenson Jr., Prog. Part. Nucl. Phys. 12 (1984) 409.
- [13] M. Doi, T. Kotani and E. Takasugi, Prog. Theor. Phys. 83 (1985) 1.
- [14] A.S. Barabash et al., Phys. Lett. B 249 (1990) 186.
- [15] A.S. Barabash et al., Proc. XIth Moriond Workshop, Tests of fundamental laws in physics (Les Arcs, Savoie, France, January 1991).  
F.T. Avignone et al., Proc. 2nd Intern. Workshop on Theoretical and phenomenological aspects on underground Physics (TAUP '91) (Toledo, Spain, September 1991).
- [16] D. Dassié et al., Proc. 2nd Intern. Workshop on Theoretical and phenomenological aspects on underground physics (TAUP '91) (Toledo, Spain, September 1991).
- [17] O. Helene, Nucl. Instrum. Methods 212 (1983) 319; A 300 (1991) 132.
- [18] Particle Data Group, J.J. Hernández et al., Review of particle properties, Phys. Lett. B 239 (1990) 1.